Influence of Icing on Bridge Cable Aerodynamics

Koss, Holger; Frej Henningsen, Jesper; Olsen, Idar

Published in:
Proceedings of the 15th International Workshop on Atmospheric Icing of Structures (IWAIS XV)

Publication date:
2013

Influence of Icing on Bridge Cable Aerodynamics

Holger Hundborg Koss [#*1], Jesper Frej Henningsen[#], Idar Olsen[#]

[#] *Department of Civil Engineering, Technical University of Denmark*
Brovej, Building 118, DK-2800 Kgs. Lyngby, Denmark
[1] hko@byg.dtu.dk

[*] *FORCE Technology*
Hjortekærsvej 99, DK-2800 Kgs. Lyngby, Denmark

Abstract — **In recent years the relevance of ice accretion for wind-induced vibration of structural bridge cables has been recognised and became a subject of research in bridge engineering. Full-scale monitoring and observation indicate that light precipitation at moderate low temperatures between zero and -5°C may lead to large amplitude vibrations of bridge cables under wind action. For the prediction of aerodynamic instability quasi-steady models have been developed estimating the cable response magnitude based on structural properties and aerodynamic force coefficients for drag, lift and torsion. The determination of these force coefficients require a proper simulation of the ice layer occurring under the specific climatic conditions, favouring real ice accretion over simplified artificial reproduction. The work presented in this paper was performed to study the influence of ice accretion on the aerodynamic forces of different bridge cables types. The experiments were conducted in a wind tunnel facility capable amongst others to simulate in-cloud icing conditions.**

I. Abbreviations and Nomenclature

- α - angular position of the ice layer relative to the position during accretion process [deg]
- C_D - aerodynamic drag force coefficient [-]
- C_L - aerodynamic lift force coefficient [-]
- CWT - collaborative Climatic Wind Tunnel facility
- F_D - aerodynamic drag force [kN]
- F_L - aerodynamic lift force [kN]
- HDPE - high-density polyethylene
- I_u - turbulence intensity of along wind component [%]
- LWC - liquid water content [g/m^3]
- MVD - median volume diameter [μm]
- u - wind tunnel airspeed [m/s]
- θ - angle for lift force antisymmetry axis [deg]
- R_a - average surface roughness [μm]
- Re - Reynolds number based dry tube diameter [-]
- Re_{cr} - critical Reynolds number [-]

II. Introduction

A. Background and Aim of the Study

Bridge cables are subjected to static and dynamic loading. The static loading mainly originates from by the weight of the bridge deck, the traffic load, time averaged wind action and from the dead weight of the cable itself. For inclined cables, the additional effect from pre-stressing to counteract the cable sag has to be considered as well. Dynamic loading on the other hand derives either from motion of the bridge structure due to traffic and wind action on the bridge deck and pylon or, more significantly, due to direct aerodynamic excitation of the cable.

Ambitious bridge projects with ever longer span widths push the capacity of structure and material to the limit. Presently the world's largest suspension bridges in terms of main span are the Akashi Kaikyo Bridge (Japan, 1998) with 1,991m, Xihoumen Bridge (China, 2009) with 1,650m and the Great Belt Bridge (Denmark, 1998) main span is 1,624m long. The largest cable-stayed bridges are the Sutong Bridge (China, 2008) with 1,088m, the Stonecutters Bridge (Hong Kong, 2009) with 1,018 and the Tatara Bridge (Japan, 1999) has a main span of 890m. The 2006 proposal for the Messina Bridge considered a single-span suspension bridge with a central span of 3,300m.

The large stay planes of long-span bridges can now produce more than 50% of the overall horizontal load on a bridge [1]. For this reason cover tubes of the structural cables are equipped with different types of surface patterns which beside mitigation of vortex shedding and rain-wind induced vibrations also reduce the aerodynamic drag forces at design wind velocities. Kleissl and Georgakis [2] performed a comparative study on three different cover tube types for bridge cables focusing on drag and lift forces and on the related aerodynamic effects at the tube surface in configurations perpendicular and inclined to the wind. The uniqueness of this study is the fact that the tests on all tube specimens were conducted in the same facility hence eliminating systematic errors due to different flow conditions or experimental setup for the comparison.

Knowing how the aforementioned cable types perform in dry and rain conditions this paper focuses on how much ice accretion alters the aerodynamic behaviour of these cable types.

B. Bridge Cable Tubes

The study of ice accretion effects on the cable aerodynamics was performed on the same tube types as used and described in [2]: (a) a plain HDPE tube, (b) a HDPE tube fitted with helical fillets and (c) a HDPE tube with a pattern-indented surface (Fig. 1).

The sectional models are original full-scale samples, supplied by bridge cable manufacturers. The plain HDPE tube has 160mm outer diameter and a measured average surface roughness of $R_a \approx 1.8$μm. The HDPE tube with two helically

wrapped fillets has an outer diameter of 160 mm as well. The fillets are rounded with a height of approximately 3mm and a base width of approximately 4 mm. Furthermore, they have a 3.14 tube diameter pitch length (502mm and 45°). The average material surface roughness is in the order of $R_a \approx 3.0\mu m$. The pattern-indented tube has a diameter of 140mm, and is an actual sample of the most common diameter of cable used on the Sutong Bridge. The relative surface roughness is defined by the depth of the indentations, measured to be approximately 1% of cable diameter.

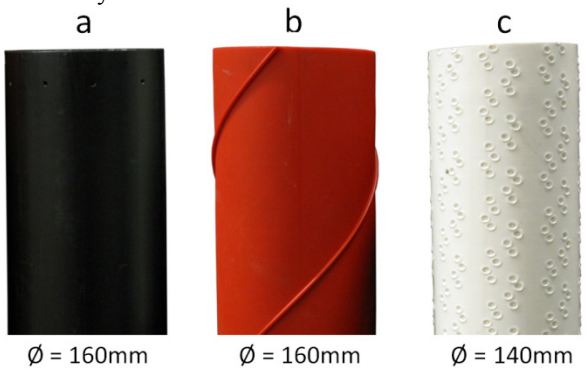

Fig. 1. Bridge cable cover tubes tested in the ice accretion study: (a) a plain HDPE tube, (b) tube wrapped with two helical fillets, (c) a tube with a pattern-indented surface texture.

The relevance of using original cover tubes instead of recreations is documented in studies focusing on the influence of surface roughness and non-circularity on aerodynamic force coefficients [3]. Especially the lift coefficient is sensible to surface roughness irregularities and cross-sectional distortion.

C. Reference Aerodynamic Performance

The aerodynamic performance of the three cable tubes shown in Fig. 1 have been studied and reported in [2]. Fig. 2 shows the development of the drag force coefficient, C_D, over Reynolds number.

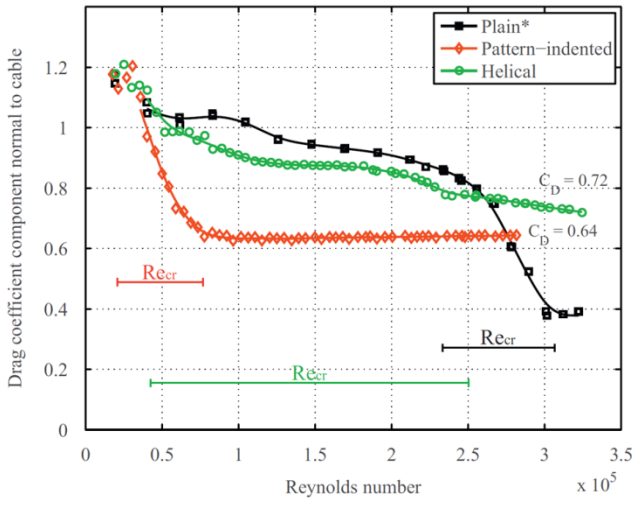

Fig. 2. Drag force coefficient, C_D, as function of Reynolds number for the three cable types in dry condition and flow normal to cable axis. For each cable type the corresponding critical range of significant drag force reduction is indicated [2]. Maximum turbulence intensity $I_{u,max} = 0.6\%$.

For the same flow conditions the lift coefficients, C_L, for the three cable types are shown in Fig. 3 as a function of Reynolds number. As shown in [3] the lift force on the plain cable tube is very susceptible to surface roughness and the measured result varies significantly on the angle of attack, α, even for wind normal to cable axis (cross-flow condition).

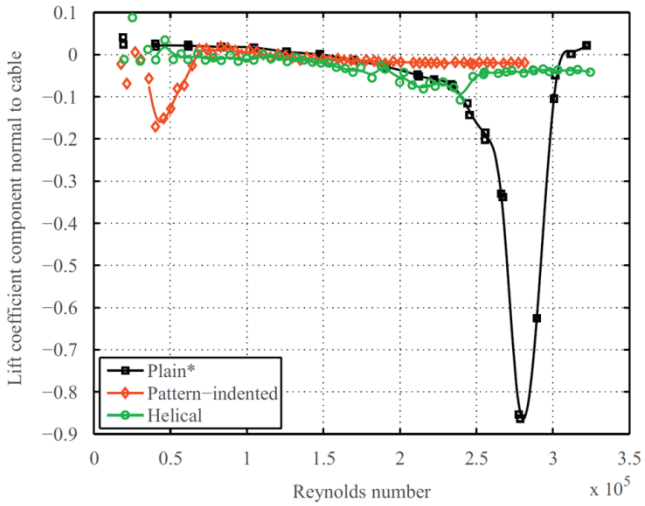

Fig. 3. Lift coefficient, C_L, as function of Reynolds number for the three cable types in dry condition and flow normal to cable axis [2]. Maximum turbulence intensity $I_{u,max} = 0.6\%$.

III. Experimental Setup & Test Conditions

The tests were performed in the collaborative Climatic Wind Tunnel (CWT) at FORCE Technology in Lyngby, Denmark. The wind tunnel was developed and built between 2008 and 2010 as a joint project between the Technical University of Denmark (DTU), FORCE Technology funded by the Danish bridge owners/operators Femmern Bælt A/S and Storebælt A/S.

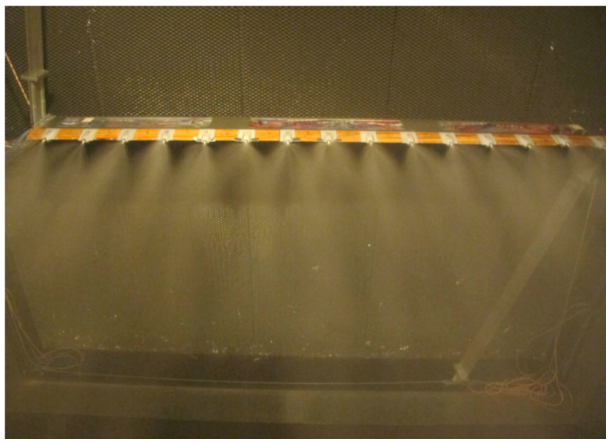

Fig. 4. Horizontally mounted 15 nozzle spray bar operating in the settling chamber of the wind tunnel to simulate in-cloud icing conditions [5].

The main technical specifications are: 5m long test chamber with a cross-section of 2 x 2m, maximum airspeed $u_{max} = 32m/s$, lowest turbulence intensity is $I_{u,min} = 0.6\%$. The lowest long-term average temperature at full speed is -4.5°C. The blockage ratio for a 160mm diameter cable segment is about 8%. Further information is available in [4].

Heart of the CWT is the cooling system capable of operating the facility at sub-zero air temperatures and the recently developed spray system allows for creation of in-cloud icing conditions. Fig. 4 shows the spray bar with 15 nozzles producing droplets in the size range between 10 and 80µm (median volume diameter, *MVD*) depending on the air/water pressure ratio and magnitude. The spray bar can be rotated steplessly to assume any position for testing inclined cables ([5], [6], [7]).

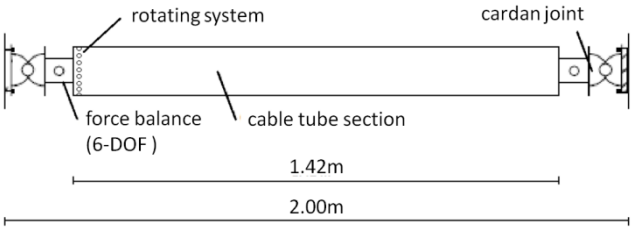

Fig. 5. Arrangement of force balances, cable tube tests specimen and connectors horizontally mounted in the middle of the test section to capture the aerodynamic loads for varying airspeed and rotation angle α.

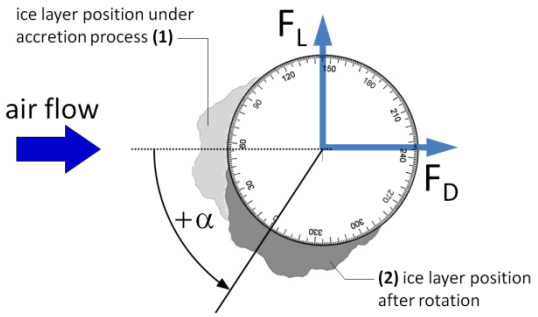

Fig. 6. Orientation of drag and lift forces. The angle of rotation α (counter-clockwise) corresponds to the clockwise relative angle of attack.

Fig. 5 illustrates the arrangement of the cable test specimen, the two 6-component AMTI MC3A-500 force balances on each side of the cable and the joint connections to the wind tunnel walls to avoid end-moment effects. The cable tube can be rotated in steps of $\Delta\alpha = 10°$ around its length axis. The corresponding lift and drag force coordinate system is shown in Fig. 6. The position of the ice layer is measured in degrees as the angular distance between its location during accretion (1) and the location during wind load testing (2) counting positive for counter-clockwise rotation.

In 2009 a fundamental study on ice accretion on circular cylinders at moderate low temperatures was performed at the National Research Counsil (NRC) in Ottawa, Canada [8]. 'Moderate low temperatures' refer to air temperatures between 0 and -5°C at which ice accretion and subsequent large amplitude wind-induced vibrations have been observed on bridges in the past. This temperature range can be divided into three sub-ranges: high moderate temperatures (0 to -2°C) characterised by wet ice accretion (glaze), low moderate (-3 to -5°C) with dry ice (rime) and a transition range around -3°C with a mixed ice type. In this study ice accretion in the high and low temperature range has been simulated with target temperatures of -2 and -5°C for wet and dry ice, respectively.

TABLE I summarises the boundary conditions of the simulations including the measured ice mass after 60 minutes of accretion. The airspeed during icing was $u = 10.5$m/s with a maximum along-wind turbulence intensity of $I_u = 0.6\%$.

TABLE I
SIMULATION CONDITIONS: SETTINGS AND ACHIEVED VALUES

cable tube type	icing condition	ID	mean air temp.	accretion time	MVD[1]	LWC[2]	ice mass
		[-]	[°C]	[min]	[µm]	[g/m³]	[kg/m]
a) standard plain	wet	SW	-2.0	60	10-15	0.4	0.60
	dry	SD	-5.1	60	10-15	0.4	0.56
b) helical fillet	wet	HW	-2.2	60	10-15	0.4	0.46
	dry	HD	-5.1	60	10-15	0.4	0.49
c) pattern-indented	wet	PW	-1.8	60	10-15	0.4	0.53
	dry	PD	-5.3	60	10-15	0.4	0.60

[1] The MVD is estimated based on nozzle specification provided by the manufacturer using the air/water pressure ratio and magnitude.
[2] The LWC of 0.4g/m³ is a target value. Comparison tests indicate that the true value might be higher by 30%.

Even though horizontal orientation is untypical for bridge cables the tube specimens were mounted horizontally for comparison with the observation data base from the NRC tests regarding the ice accretion characteristics [8]. Furthermore, the orientation allowed for dynamic testing of galloping instability in a simple free vibration setup for vertical cross-flow vibrations [5].

IV. EVALUATION CONSIDERATIONS

The influence of the ice layer on the aerodynamic performance of the bridge cable tubes is in this study evaluated based on the drag and lift coefficients as a function of the rotation angle α and the applied airspeed *u* or Reynolds number Re, respectively. With a counter clockwise rotation α as shown in Fig. 6 the resulting angle of attack is measured positive in clockwise direction starting from the stagnation line of dry tube at the beginning of the accretion process (identical to α). The evaluation will focus on:

- development of C_D and C_L over rotation angle α
- dependency of C_D and C_L on Reynolds number
- influence of ice layer on symmetry of C_D
- influence of ice layer on antisymmetry of C_L
- influence of gravity on icing.

An ice layer perfectly symmetric around the stagnation point during the accretion process will be reflected by a symmetric drag force curve $C_D(\alpha)$ and an antisymmetric lift force curve $C_L(\alpha)$. Each deviation from this rule is due to irregularity of the ice layer in practice. A larger influence on the symmetry can be expected from gravity during the accretion process – in particular for wet ice accretion.

Fig. 7 shows a simplified example on an ice layer that due to gravity exhibits an asymmetry around the flow direction during the accretion process (1): the ice mass is shifted towards the underside of the cable. In this simplified case it appears that there is an axis around which the ice layer is still (almost) symmetric. The location of this axis is defined by the angle θ and for airflow along this axis the lift force should be zero: $C_L(\alpha = -\theta) \approx 0$. In this sense θ can also be interpreted as the *dominating angle for neutral lift* serving as a measure for gravity influence on ice accretion.

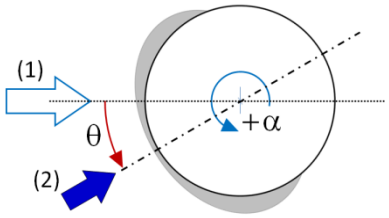

Fig. 7. Ice accretion under influence of gravity: the ice mass is shifted towards the underside of the cable tube. A symmetry axis can be found at an angle of θ around which the ice layer is (nearly) symmetric and the lift force (nearly) antisymmetric, depending on the irregularity of the ice layer.

The influence of icing affected by gravity on the aerodynamic performance is evaluated using the principle of lift force antisymmetry in a graphical approach illustrated in Fig. 8. An antisymmetric image of the measured lift curve, $C_L(\alpha)$, is projected on the measured data and shifted along the abscissa axis to find (graphically) the best match. The resulting shift angle equals 2θ.

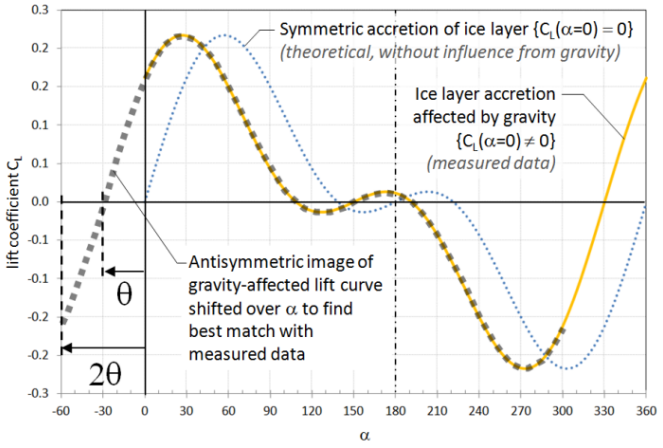

Fig. 8. Graphical method to estimate the influence of gravity on the ice accretion and on the resulting lift force. An antisymmetric image of the lift force coefficient curve is superimposed with itself to find the best match.

In practise, ice accretion affected by gravity exhibits large irregularity and asymmetry. For this reason 'the best match' may only be applicable to some features of the lift curve. The poorer the congruence between the measured lift curve and its antisymmetric image the less dominant is the identified angle for neutral lift. In extreme case θ marks only one out of many possible neutral directions.

V. Standard Plain Cable

A. Wet Ice Accretion (SW)

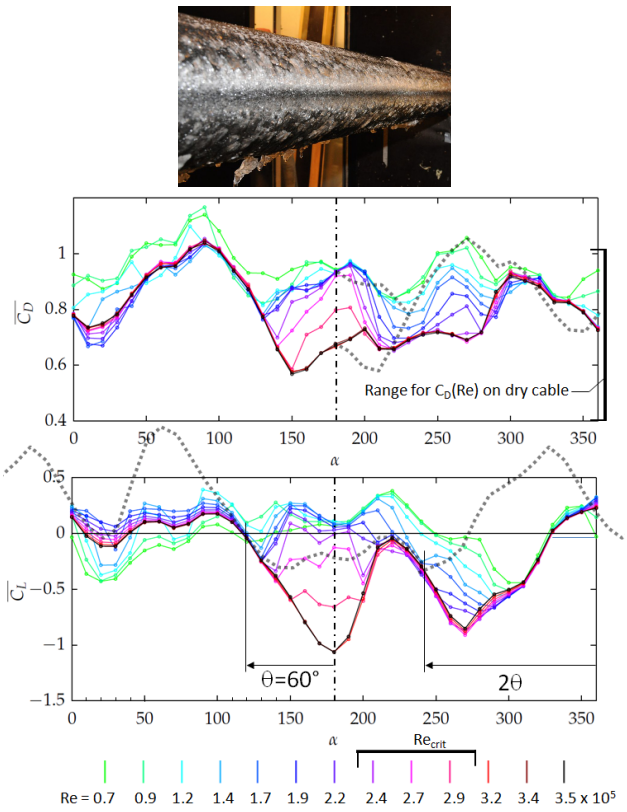

Fig. 9. Drag and lift coefficients of standard plain cable tube for wet ice accretion (Accretion time: 60min; mean air temperature: -2°C; ice mass: 0.6kg/m).

The ice layer exhibits a high irregularity hence the antisymmetric image of the lift curve matches the measured data only in few features. The resulting dominant angle for neutral lift at α = 120°, i.e. from rear below. The poor match in the lift curves indicates that gravity influences the wet ice accretion on the plain standard cable significantly.

The high irregularity affects the drag force as well. Expecting a curve mirrored around α = 180° (grey dotted line) only a vague resemblance between both sides can be observed. For some angles of attack the drag force of the iced plain cable still exhibits a Reynolds dependency as measured on the dry cable (Fig. 2). For other angles the dependency of C_D almost disappears. With the ice layer near the flow separation points the cable assumes a sharp-edged body characteristic.

It seems that the ranges of flow angles with a high Reynolds dependency of C_D are similar to those where C_L varies with Reynolds number as well.

In Fig. 9 the range for the drag coefficient measured on the dry cable (left graph border) and the corresponding critical Reynolds range are indicated for comparison purpose. Around α = 180° the critical Reynolds range of the iced cable is similar to the dry cable. As one could expect, the drag coefficient is generally higher on the iced cable but stays largely within the drag range of the dry cable.

B. *Dry Ice Accretion (SD)*

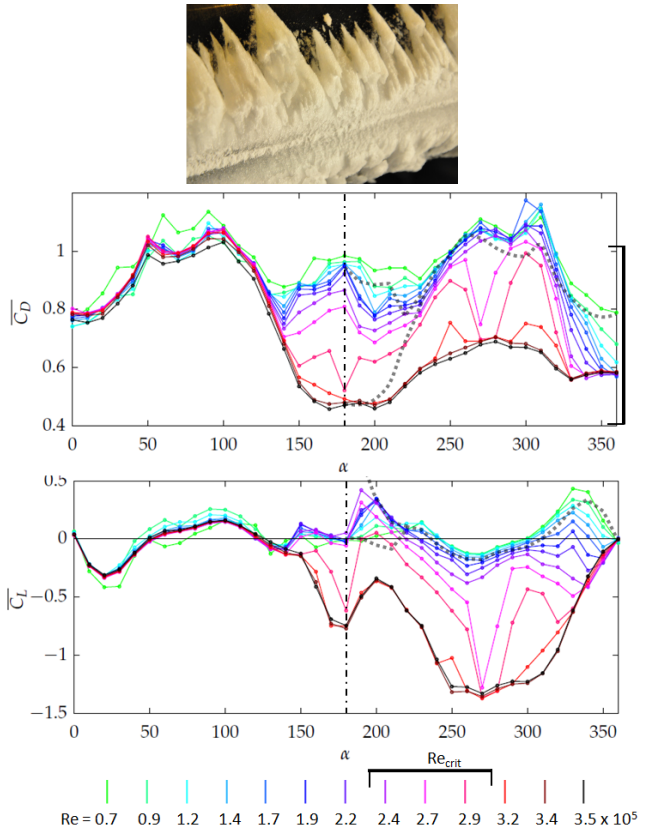

Fig. 10. Drag and lift coefficients of standard plain cable tube for dry ice accretion (Accretion time: 60min; mean air temperature: -5.1°C; ice mass: 0.56kg/m).

For dry ice accretion the ice layer is more concentrated around the stagnation line on the upstream side of the cable tube. For up to $\alpha = 120°$ the drag force is little affected by the Reynolds number indicating a rather sharp-edged body behaviour than of a circular cylinder. Between 120° and 180° the drag force is strongly dependent on Re. Here, the ice layer is fully immersed in the separated wake flow on the rear side of the cable and the tube appears aerodynamically similar to a dry cylinder with the characteristic critical Reynolds regime.

Around 180° the drag coefficient C_D is quite symmetric. This symmetry however does not extend to flow direction beyond 210°, where, according to observations below 120°, the drag force should become again independent of Reynolds number. A reason for this asymmetry of $C_D(\alpha)$ is a change in the surface roughness during the course of testing. Under dry ice accretion simulation fine spray dust creates small ice flake accumulation on the rear side of the cable surface. These flakes get blown off at higher airspeeds when directly exposed to the approaching wind. As a consequence the surface roughness is changed in the second half of the tests clearly affecting the Reynolds dependency for both drag and lift force.

VI. Helical Fillet Cable

A. *Wet Ice Accretion (HW)*

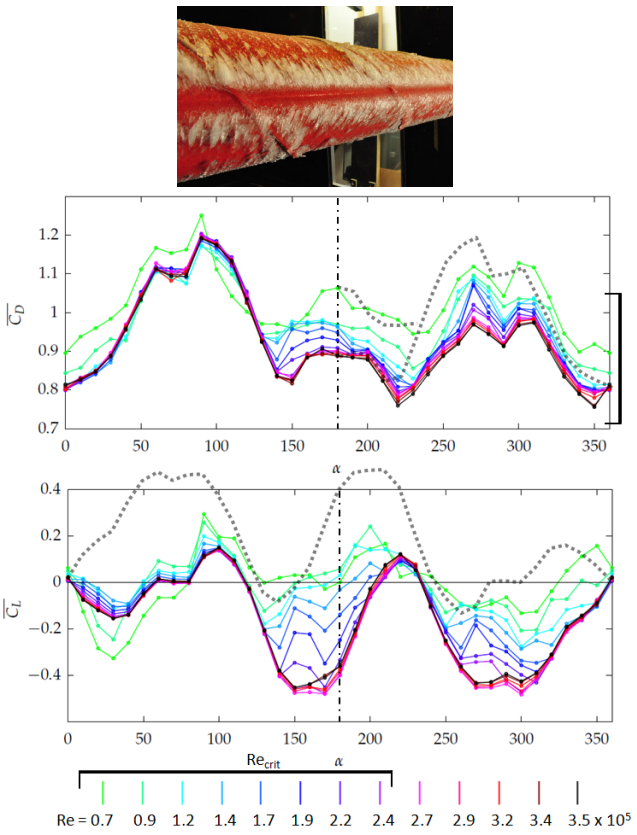

Fig. 11. Drag and lift coefficients of helical fillet cable tube for wet ice accretion (Accretion time: 60min; mean air temperature: -2.2°C; ice mass: 0.46kg/m).

The drag force coefficient is reasonably symmetric around $\alpha = 180°$. Similar to the observation on the plain cable C_D is fairly Reynolds number independent up until 130°. Hereafter the ice layer enters the wake flow and the cable assumes an aerodynamic behaviour closer to dry cable conditions. The symmetry of the drag force is influenced by the irregularity of the ice layer. This is in particular reflected by the increased level of Reynolds dependency for relative flow direction above 180°.

The wet ice layer covers a larger part of the cable tube surface hence influencing the airflow along the tube surface even if the main part of the ice is in the wake flow zone. For this reason the drag coefficient reaches only for some specific angles the low drag level of the dry cable. When the ice layer is near the separation point, i.e. around 90° or 270°, the drag coefficient peaks and exceeds the level of the dry cable up to 15%.

Comparing the lift force coefficient curve with its antisymmetric image indicates a very low level of ice layer symmetry. Both curves show a certain resemblance to each other but differ significantly in magnitude.

B. *Dry Ice Accretion (HD)*

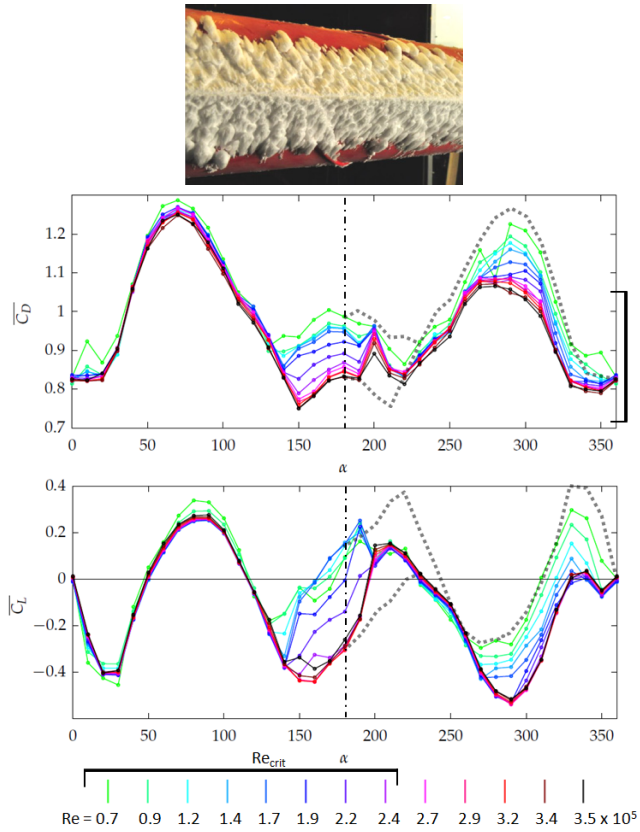

Fig. 12. Drag and lift coefficients of helical fillet cable tube for dry ice accretion (Accretion time: 60min; mean air temperature: -5.1°C; ice mass: 0.49kg/m).

As observed on the standard plain cable tube the ice accretion is more concentrated around the stagnation line compared to wet ice. Both drag and lift coefficient curves indicate a reasonable symmetry allowing for some irregularity.

The influence of the ice layer on the drag coefficient magnitude is higher than observed from wet ice accretion. For ice layer positions near flow separation (around 90° or 270°) C_D peaks 1.28, approximately 20% above the maximum drag of the dry cable tube.

According to Fig. 2 the dry cable exhibits a wide critical range. On the iced cable this dependency appears for relative flow direction placing the ice layer in the wake flow zone of the cable tube ($130° < \alpha < 230°$). The symmetry of the drag curve is influenced by the natural irregularity of the ice layer and by the change of surface roughness throughout the test as discussed for the standard plain cable. The influence of the surface roughness change seems to be smaller on the helical fillet tube than on the plain cable. The fillets define at discrete positions the location of flow separation hence 'damping' the Reynolds number dependency.

As discussed above the lift coefficient curve shows a reasonable antisymmetry. The variation of C_L with Reynolds number seems to follow the pattern observed for C_D.

VII. PATTERN-INDENTED CABLE

A. *Wet Ice Accretion (PW)*

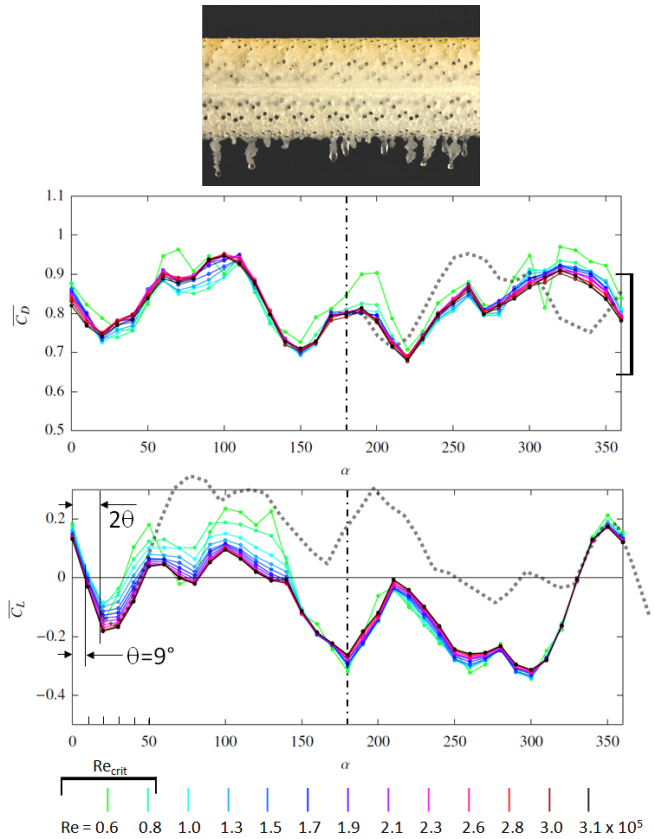

Fig. 13. Drag and lift coefficients of pattern-indented cable tube for wet ice accretion (Accretion time: 60min; mean air temperature: -1.8°C; ice mass: 0.53kg/m).

A main feature in the aerodynamic performance of the pattern-indented cable is the low drag coefficient almost constant in the supercritical range starting at a relatively low Reynolds number (Fig. 2). The C_D range of the dry cable over the Reynolds range applied in this study is indicated to the right in upper graph of Fig. 13. As it appears, the drag coefficients of the iced cable stay inside the dry cable drag range but reach only for few relative flow directions the characteristic low drag level.

However, the pattern-indented cable tube exhibits even with wet ice a very low Reynolds dependency of the drag force for all tested relative flow directions. This behaviour distinguishes the pattern-indented cable clearly from the standard plain and helical fillet cable.

The increased ice mass on the underside of the cable tube (e.g. icicles, shown in the photograph of Fig. 13) creates some irregularity and asymmetry in the ice layer leading to a limited symmetry of the drag curve.

The lift force curve shows for some flow directions a certain variation at low Reynolds numbers. Antisymmetric resemblance is limited and characterised by a difference of lift force coefficients as seen in case HW.

B. *Dry Ice Accretion (PD)*

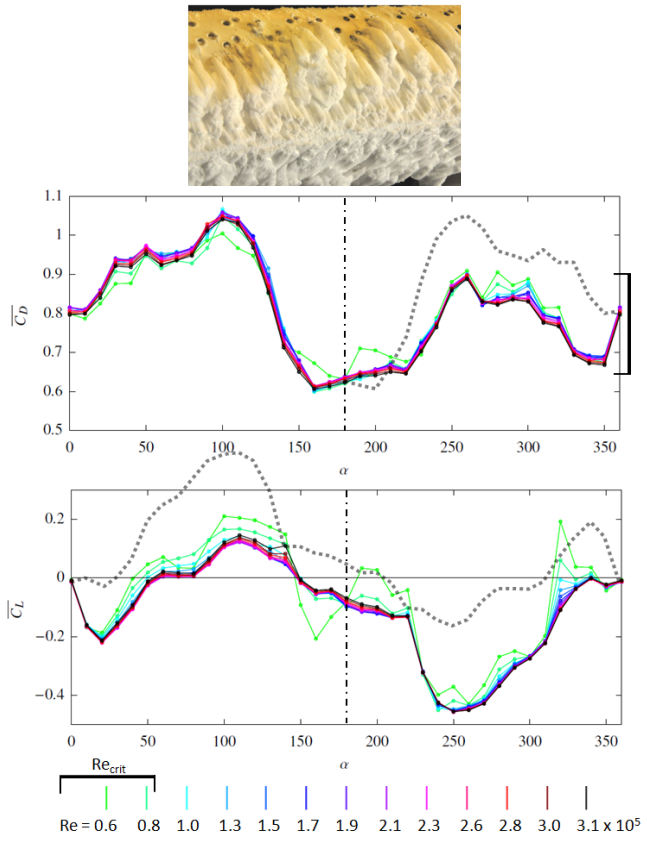

Fig. 14. Drag and lift coefficients of pattern-indented cable tube for dry ice accretion (Accretion time: 60min; mean air temperature: -5.3°C; ice mass: 0.6kg/m).

The dry ice layer changes the drag force of the pattern-indented cable stronger than observed for wet ice. The drag coefficients exceed the dry cable values by about 15% for flow directions where the ice layer is near the flow separation point.

The effect of ice layer and wake flow and the change of surface roughness on the drag force are similar to the dry ice accretion on the other cable types. Still, main characteristic is the very low dependency on the Reynolds number for all investigated angles α.

The lift force coefficient curve indicates a high irregularity but is, apart from lower airspeeds, Reynolds number independent.

VIII. CONCLUSION

The influence of icing on bridge cable aerodynamics was investigated on three different original full-scale samples of bridge cable cover tubes (standard plain, helical fillet and pattern-indented) for two different types of ice accretion (wet and dry). The tests were performed in specially built wind tunnel facility allowing for simulating in-cloud icing conditions.

The observation from the ice accumulation after 60min accretion time can be summarized to:

- *Wet ice*: the ice layer consists mainly of glaze ice exhibiting a noticeable asymmetry with increased ice mass on the underside of the cable due to gravity.
- *Dry ice*: consisting of rime ice apparently symmetric around stagnation line during accretion phase. Spray dust creates small ice flakes on the rear side of the cable tube surface.

With respect to the influence of the ice layer on aerodynamic performance of the three cable types following main conclusion can be drawn:

- The standard plain cable is most affected by ice accretion with respect to sensibility of drag to Reynolds number, to the magnitude of lift coefficient and to the sensibility of both force coefficients to surface roughness.
- Both helical fillet and pattern-indented cable are less susceptible to changes of the cable surface and ice accretion where the pattern-indented is least affected.
- The pattern-indented cable seems to cope best with the effect of ice accretion. For comparable icing conditions the pattern-indented cable has lower overall drag and lift coefficients compared to standard plain and helical fillet cable.

As an extension of the here presented work the susceptibility to aerodynamic instability was investigated using the Den Hartog criterion for galloping. Preliminary results indicate that under the given conditions only the plain standard cable exhibited tendencies for instability.

REFERENCES

[1] N.J. Gimsing and C.T. Georgakis, *Cable Supported Bridges: Concept and Design*, 3rd ed. John Wiley & Sons Ltd., 2011.

[2] K. Kleissl and C.T. Georgakis, *Comparison of the aerodynamics of bridge cables with helical fillets and a pattern-indented surface*, Journal of Wind Engineering and Industrial Aerodynamics, vol.104-106, 2012, pp.166-175

[3] G. Matteoni and C.T. Georgakis, *Effects of bridge cable surface roughness and cross-sectional distortion on aerodynamic force coefficients*, Journal of Wind Engineering and Industrial Aerodynamics, Vol.104-106, 2012, pp.176-187

[4] C.T. Georgakis, H.H. Koss and F. Ricciardelli, *Design Specifications for a Novel Climatic Wind Tunnel for the Testing of Structural Cables*. Proceedings 8th International Symposium on Cable Dynamics, 2009, Paris, France

[5] H.H. Koss and M.S.M. Lund, *Experimental Investigation of Aerodynamic Instability of Iced Bridge Sections*, In: 6th European and African Conference on Wind Engineering, Robinson College, Cambridge, UK, 2013.

[6] C. Demartino, H.H Koss and F. Ricciardelli, *Experimental study of the effect of icing on the aerodynamics of circular cylinders – Part I: Cross flow*. In: 6th European and African Conference on Wind Engineering, Robinson College, Cambridge, UK, 2013.

[7] C. Demartino, C.T. Georgakis and F. Ricciardelli, *Experimental study of the effect of icing on the aerodynamics of circular cylinders – Part II: Inclined flow*. In: 6th European and African Conference on Wind Engineering, Robinson College, Cambridge, UK, 2013.

[8] H.H. Koss, H. Gjelstrup, C.T. Georgakis, *Experimental study of ice accretion on circular cylinders at moderate low temperature*., Journal of Wind Engineering and Industrial Aerodynamics, Vol.104-106, 2012, pp.540-546.